Int. J. Engng Ed. Vol. 10, No. 2, pp. 201–207, 1994
Printed in Great Britain.

0742-0269/91 $3.00+0.00

Convolutions, Transforms and Edge Detection in Images*

JOHN SCHMEELK
Department of Mathematical Sciences, Virginia Commonwealth University, Richmond, Virginia, VA 23284-2014 USA

Student motivation in mathematical courses continue to be a major concern. The author argues that a partial solution to this problem is to offer some stimulating elementary image processing techniques that will provide the student with immediate visual examples implementing profound mathematical theory. This paper will offer very elementary applications for mathematical concepts that are often difficult to convey. They will include convolution, Fourier transforms and filtering. The mathematics is contained in the paper and stresses its application to the image. The paper also contains a very brief introduction on wavelet theory, which is becoming a very innovative method in understanding many difficult discrete data files.

1. INTRODUCTION

STUDENT motivation in mathematical courses continues to be a major concern. The students in a calculus, linear algebra, or matrix analysis course often experience motivational problems contributable in part to the apparent shortage of relevance of the course material to their immediate interests and personal experiences. The author argues that a partial solution to this problem is to offer some stimulating elementary image processing techniques that will provide the student with immediate visual examples implementing profound mathematical theory.

To this end this paper provides an introduction to some interesting problems in image processing and describes some unusual applications for convolutions, frequency analysis, matrices, and partial derivatives [1–5]. The applications are all drawn from image enhancement and are at a level of undergraduate mathematics [6–9]. Depending on the text being studied in the calculus, linear algebra and matrix theory course, some portions of our techniques may be included in third or fourth semester applications.

One principle application to be addressed will be that of edge detection [4, 9–11]. It has far-reaching results in many applications to include computer vision, human vision and several innovative medical techniques [12–14]. For example, a patient suffering from an aneurysm may be diagnosed through an angiogram. An angiogram is a pictorial illustration of the blood vessels having edges highlighted through the implementation of mathematical edge enhancement [4, 11]. The visible edges can be studied by the physician and a diagnosis of the condition can be completed with greater accuracy.

Many image enhancement processes are performed and computed using mathematical convolutions, spatial and frequency filters in conjunction with several mathematical transform algorithms. Recently new transforms are being implemented, drawing from the theory of wavelets. We will conclude the paper with the definition and application of a 'mother' wavelet. Several sources will be given for the application of these techniques when they are applied to image enhancement.

2. SOME NOTIONS AND NOTATIONS

Since a flat image is contained within a two-dimensional Euclidean space, our featured space will be $\mathbb{R}^2$. We will recall several fundamental definitions and results for $\mathbb{R}^2$. For convenience, we select two sets of continuous spatial coordinates by the somewhat unusual notation

$$x=(x_1, x_2) \text{ and } y=(y_1, y_2)$$

where $x_j, x_i\ (1 \leqslant i \leqslant 2)$ are elements belonging to the set of real numbers, $\mathbb{R}$. The familiar dot product formula then becomes

$$x \circ y = \sum_{i=i}^{2} x_i y_i$$

together with its corresponding induced norm,

$$\|x\| = + \sqrt{\sum_{i=i}^{2} x_i^2}$$

Implementing trigonometry, it is easily shown that the cosine of the angle, ϕ, between two vectors determined by their spatial coordinates, x and y, is in fact

$$\cos\phi = \frac{x \circ y}{\|x\| \cdot \|y\|}$$

* Paper accepted 10 April 1994.

provided $\|x\| \neq 0$ and $\|y\| \neq 0$ or

$$x \circ y = \|x\| \cdot \|y\| \cdot \cos(\phi) \tag{2.1}$$

Expression (2.1) immediately indicates that perpendicular vectors will have a dot product equal to zero and normalized colinear vectors will have a dot product equal to one. This observation is important in Section 3.

We now revisit the partial derivative definitions,

$$\frac{\partial f(x_1, x_2)}{\partial x_1} = \lim_{\Delta x_1 \to 0} \frac{f(x_1 + \Delta x_1, x_2) - f(x_1, x_2)}{\Delta x_1} \tag{2.2}$$

and

$$\frac{\partial f(x_1, x_2)}{\partial x_2} = \lim_{\Delta x_2 \to 0} \frac{f(x_1, x_2 + \Delta x_2) - f(x_1, x_2)}{\Delta x_2}$$

When we examine a computer image on a monitor using a reasonable number of pixel locations illustrating the image would be 256 rows and 256 columns of pixel locations. This then defines a grid size of 256×256 square. The location of a particular pixel can then be designated using the cartesian coordinate (n_1, n_2), where n_1 is the row location and n_2 is the column location. Clearly in this application the set of values for n_i, $1 \leqslant i \leqslant 2$, would range over positive integer values. If we further normalize the distance between pixel locations, then $\Delta x_1 = \Delta x_2 = 1$ and our discrete approximate partial derivative formulas at the pixel locations become

$$\frac{\partial f(n_1, n_2)}{\partial n_1} \approx \frac{f(n_1 + 1, n_2) - f(n_1, n_2)}{1}$$
$$= f(n_1 + 1, n_2) - f(n_1, n_2) \tag{2.3}$$

and

$$\frac{\partial f(n_1, n_2)}{\partial n_2} \approx \frac{f(n_1, n_2 + 1) - f(n_1, n_2)}{1}$$
$$= f(n_1, n_2 + 1) - f(n_1, n_2)$$

3. THE GRADIENT

We now introduce the notion of a directional derivative for a function, $f(x_1, x_2)$ at a point $(a, b) \varepsilon \mathbb{R}^2$ evaluated in the direction, L. The direction, θ, of L was chosen and the equations,

$$x_1 = a + r \cos\theta$$
$$x_2 = b + r \sin\theta$$

will be implemented, where r ranges over the real numbers $\leqslant 0$. Figure 1.1 illustrates the vector, L.

We introduce the classical definition for the gradient of the function, $f(x_1, x_2)$ to be

$$\nabla f = \left(\frac{\partial f(x_1, x_2)}{\partial x_1}, \frac{\partial f(x_1, x_2)}{\partial x_2} \right) \tag{3.2}$$

together with a unit vector in direction, θ to be

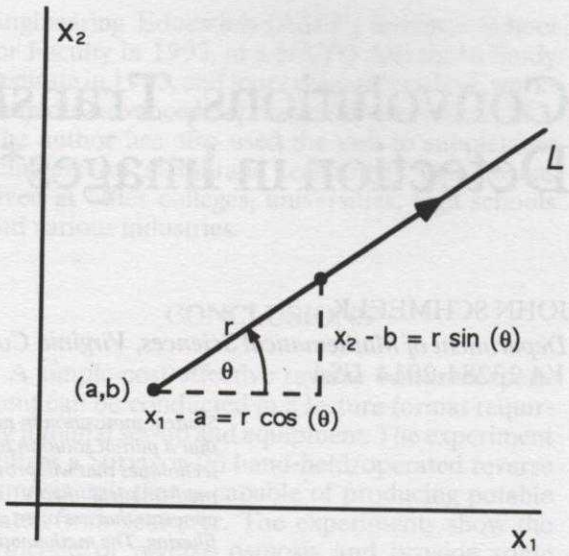

Fig. 1. Directional derivative.

$$u = (\cos\theta, \sin\theta) \tag{3.3}$$

We assume the chain rule and compute the directional derivative of $f(x_1, x_2)$ at (a, b) in the direction given by the vector, L. Implementing formulas (3.1)–(3.3), these computations become

$$\left. \frac{df(a + r\cos\theta, b + r\sin\theta)}{dr} \right|_{r=0}$$
$$= \left. \frac{\partial f}{\partial x_1} \frac{\partial x_1}{\partial r} + \frac{\partial f}{\partial x_2} \frac{\partial x_2}{\partial r} \right|_{r=0}$$
$$= \frac{\partial f(a, b)}{\partial x_1} \cos\theta + \frac{\partial f(a, b)}{\partial x_2} \sin\theta$$
$$= \left(\frac{\partial f(a, b)}{\partial x_1}, \frac{\partial f(a, b)}{\partial x_2} \right) \circ (\cos\theta, \sin\theta)$$
$$= \nabla f \circ u$$
$$= \|\nabla f\| \cdot \|u\| \cdot \cos\phi$$
$$= \|\nabla f\| \cdot L \cdot \cos\phi \tag{3.4}$$

Expression (3.4) implements expression (2.1) where the angle, ϕ, is between the vector, u, and the gradient vector, ∇f. It is not to be confused with the direction of L, which is θ. It is then easily seen from expression (3.4) that the maximum value occurs when the angle, ϕ, is zero degrees; namely, the maximum value of the change of the function, $f(x_1, x_2)$ occurs in the direction of the gradient.

When we study an image and compute the change in pixel values the above result tells us that the expected greatest rate of change would be in the direction of the gradient. Using the discrete approximations given by expression (2.3), this then becomes horizontal and vertical differences between neighbouring pixel values.

4. SINGULAR MATRICES AND EDGE DETECTION

We introduce the continuous calculus definition for convolution [3–6] given by the familiar formula

$$h(x_1, x_2) * f(x_1, x_2) = \int_{-\infty}^{\infty} \int_{-\infty}^{\infty} h(y_1, y_2) f(x_1 - y_1, x_2 - y_2) dy_1 dy_2$$

and its discrete counterpart given by the formula

$$h(n_1, n_2) * f(n_1, n_2) = \sum_{k_1=-\infty}^{\infty} \sum_{k_1=-\infty}^{\infty} h(k_1, k_2) f(n_1 - k_1, n_2 - k_2)$$

We now select the singular matrix

$$h = \begin{pmatrix} 1 & 2 & 1 \\ 0 & 0 & 0 \\ -1 & -2 & -1 \end{pmatrix} \tag{4.1}$$

and convolute it with a function, $m = f(n_1, n_2)$. The function, $f(n_1, n_2)$, returns the numerical value of the gray level at a pixel location, (n_1, n_2). The value of m ranges from 0 to 255 at positive integer values, where 0 corresponds to pure black and 255 corresponds to pure white. These values do depend on the software configuration. We now compute the discrete convolution of $f(n_1, n_2)$ with the matrix, h, given in expression (4.1). This process then becomes

$$\begin{aligned} h(n_1, n_2) * f(n_1, n_2) &= \sum_{k_1=-1}^{+1} \sum_{k_2=-1}^{+1} h(k_1, k_2) f(n_1 - k_1, n_2 - k_2) \\ &= f(n_1 + 1, n_2 - 1) \\ &\quad - f(n_1 + 1, n_2 + 1) \\ &\quad + 2f(n_1, n_2 - 1) \\ &\quad - 2f(n_1, n_2 + 1) \\ &\quad + f(n_1 - 1, n_2 - 1) \\ &\quad - f(n_1 - 1, n_2 + 1) \end{aligned} \tag{4.2}$$

If we study the result given in expression (4.2), we find it represents a weighted linear sum of changes at pixel values in the vertical direction of a patch of 3×3 square array of pixel values. We thus term this result a vertical edge detector. Likewise, if we take the transpose of the matrix, h, we have

$$h^t = \begin{pmatrix} 1 & 0 & -1 \\ 2 & 0 & -2 \\ 1 & 0 & -1 \end{pmatrix}$$

which when convoluted with the image function, $f(n_1, n_2)$ will give us the weighted linear sum for the horizontal edges contained in a 3×3 square array of pixel values. Singular matrices, h and h^t, are of little utility in a mathematical environment but when applied to an image function, $f(n_1, n_2)$, enhances the edges. In fact when we compute

$$\text{edges} \triangleq + \sqrt{[h(n_1, n_2) * f(n_1, n_2)]^2 + [h^t(n_1, n_2) * f(n_1, n_2)]^2}$$

together with an imposed established threshold the so-called Sobel edge detector is produced [4, 6, 11].

We have the letters N and O illustrated in Figs 2 and 3 respectively, together with the Sobel edge detector applied to them and illustrated in Figs 4 and 5 respectively [3].

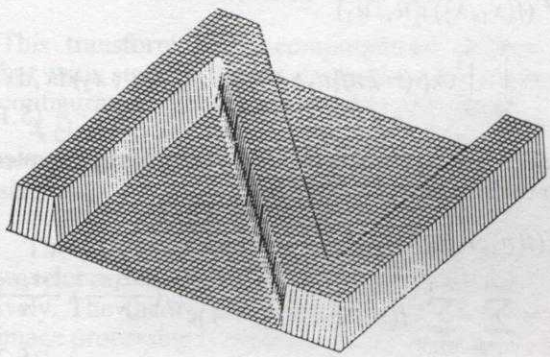

Fig. 2. The letter N.

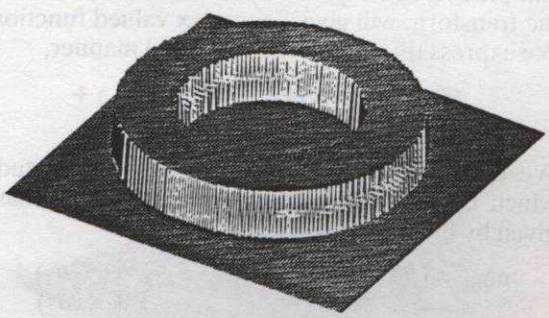

Fig. 3. The letter O.

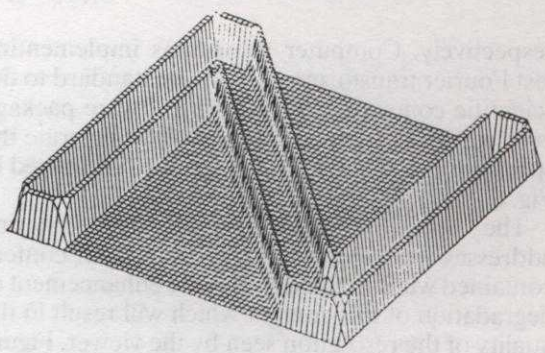

Fig. 4. Sobel edge detector on letter N.

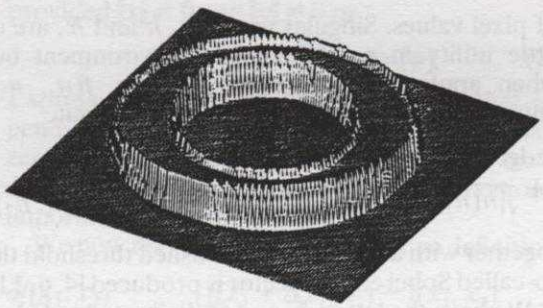

Fig. 5. Sobel edge detector on letter O.

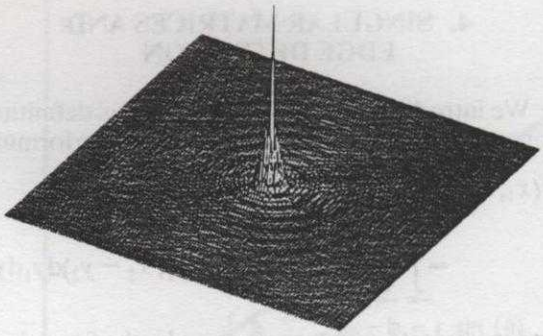

Fig. 6. Spectrum of letter O.

5. FOURIER TRANSFORM

The Fourier transform of a function [3],

$$\mathcal{F}(f(x_1, x_2))(u_1, u_2)$$
$$= \int_{-\infty}^{\infty} \int_{-\infty}^{\infty} \exp(-2\pi j[u_1 x_1 + u_2, x_2]) f(x_1, x_2) \mathrm{d}x_1 \mathrm{d}x_2 \tag{5.1}$$

and is corresponding discrete version implemented in the software, Pro-Matlab,

$$F(f(n_1, n_2))(k_1, k_2)$$
$$= \sum_{m_1=0}^{N-1} \sum_{m_2=0}^{N-1} f(m_1 + 1, m_2 + 1) \mathrm{e}^{-j\left(\frac{2\pi k_1 m_1}{N} + \frac{2\pi k_2 m_2}{N}\right)} \tag{5.2}$$

where N is of the form 2^g and g is a positive integer. Since the kernel of the Fourier transform contains a complex valued exponential function, the result of the transform will give a complex valued function. We express this function in the usual manner,

$$\mathcal{F}(f(x_1, x_2))(u_1, u_2) = U(u_1, u_2) + jV(u_1, u_2)$$

We decompose this function into its magnitude which is often called its spectrum and its phase given by the familiar formulas.

$$\mathrm{mag}[\mathcal{F}(f(x_1, x_2))(u_1, u_2)] = + \sqrt{U^2(u_1, u_2) + V^2(u_1, u_2)}$$

and

$$\mathrm{phase}\,[\mathcal{F}(f(x_1, x_2))(u_1, u_2)] = \arctan \frac{V(u_1, u_2)}{U(u_1, u_2)}$$

respectively. Computer algorithms implementing fast Fourier transform methods are standard to the scientific community. One such software package entitled Pro-Matlab has been used to illustrate the spectrum content for the letter O and illustrated in Fig. 6.

The essential technique termed filtering addresses the behaviour of the spectrum content contained within an image. It is the enhancement of degradation of this content which will result in the quality of the resolution seen by the viewer. Figure 7 illustrates a simulated defocused lens filter

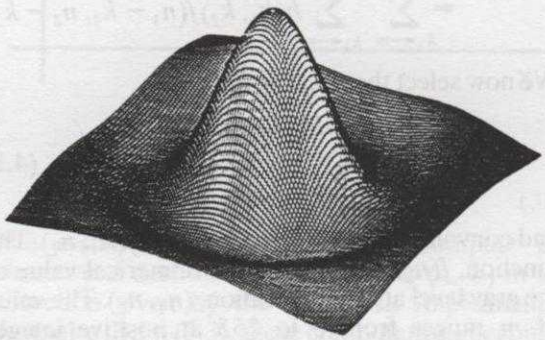

Fig. 7. Simulated defocused lens filter.

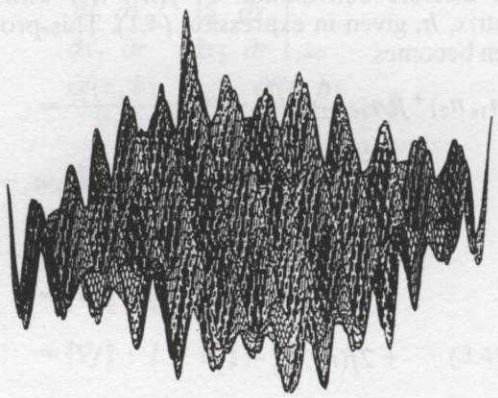

Fig. 8. Defocused letter O.

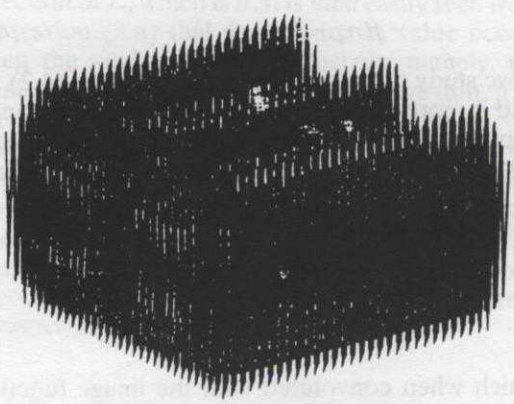

Fig. 9. Defocused letter E.

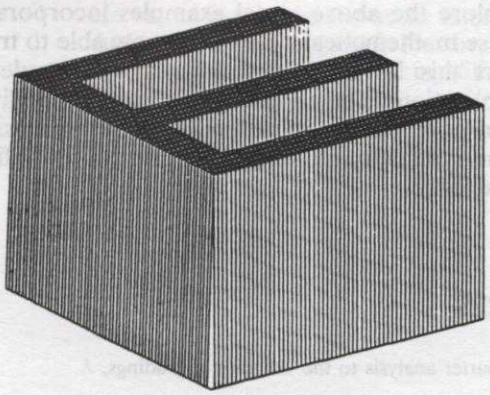

Fig. 10. Filtered and restored letter E.

constructed using mathematical formulas within the software media of Pro-Matlab. When it is applied to the letter O and E, the result is illustrated in Fig. 8 and Fig. 9 respectively. This defocused letter E can then be restored using filtering techniques as illustrated in Fig. 10. The art of filtering becomes a paramount technique to the enhancement of images in any multimedia production.

6. WAVELETS

We will restrict ourselves to wavelet functions, $\Psi(x_1, x_2)$, belonging to the class of square integrable functions usually denoted $L^2(\mathbb{R}^2)$. That is to say,

$$\int_{-\infty}^{\infty}\int_{-\infty}^{\infty} |\Psi(x_1, x_2)|^2 \mathrm{d}x_1 \mathrm{d}x_2 < \infty$$

When we select a wavelet function, $\Psi(x_1, x_2)$, having appropriate properties for the particular application, it is termed the 'mother' wavelet. We then generate a doubly indexed family of wavelets from the mother wavelet, $\Psi(x_1, x_2)$, by dialating and translating

$$\Psi^{a,b}(x) = |a_1|^{-\frac{1}{2}} |a_2|^{-\frac{1}{2}} \Psi\left(\frac{x_1 - b_1}{a_1}, \frac{x_2 - b_2}{a_2}\right)$$

where $a_i, b_i \varepsilon \mathbb{R}, a_i \neq 0, i = 1,2$.

The basic wavelet transform for the function, $f(x_1, x_2)$, with respect to the 'mother' wavelet function, $\Psi(x_1, x_2)$, then becomes

$$(\text{Wavelet } f)(a, b) = |a_1|^{-\frac{1}{2}} |a_2|^{-\frac{1}{2}}$$
$$\times \int\int \Psi\left(\frac{x_1 - b_1}{a_1}, \frac{x_2 - b_2}{a_2}\right) f(x_1, x_2) \mathrm{d}x_1 \mathrm{d}x_2.$$

We note the kernel of the Fourier transform being $\exp(-2\pi j[u_1, k_1 + u_2 k_2])$ is replaced by the translated and dialated wavelet function

$$\Psi\left(\frac{x_1 - b_1}{a_1}, \frac{x_2 - b_2}{a_2}\right)$$

There are conditions imposed on the 'mother' wavelet function, $\Psi(x_1, x_2)$, and the most natural condition is that

$$\int_{-\infty}^{\infty}\int_{-\infty}^{\infty} \Psi(x_1, x_2) \mathrm{d}x_1 \mathrm{d}x_2 = 0$$

A detailed discussion for the necessary mathematical considerations can be found in references [15–18].

Additional integer parameters, n_i, m_i $1 \leqslant i \leqslant 2$, are then included into the wavelet transform and the transform becomes

$$(\text{Wavelet } f, m, n)(a, b)$$
$$= a_1^{-m_1/2} a_2^{-m_2/2} \iint \Psi(a_1^{-m_1} x_1 - n_1 b_1, a_2^{-m_2})$$
$$\times (x_2 - n_2 b_2)\, f(x_1, x_2) \mathrm{d}x_1 \mathrm{d}x_2.$$

This transform offers computational difficulties but with state-of-the-art computer and software configurations, they can be readily computed.

A classical but important wavelet is the negative normalized second partial derivatives of the Gaussian,

$$\Psi(x_1, x_2) \exp((-x_1^2 - x_2^2)/2)$$

The Gaussian and its corresponding 'mother' wavelet are illustrated in Figs 11 and 12 respectively. The theory and application of wavelets to image processing is currently being investigated by several researchers [2, 11, 18]. The results are on the frontier of this subject and are presently being developed, reviewed and are in press.

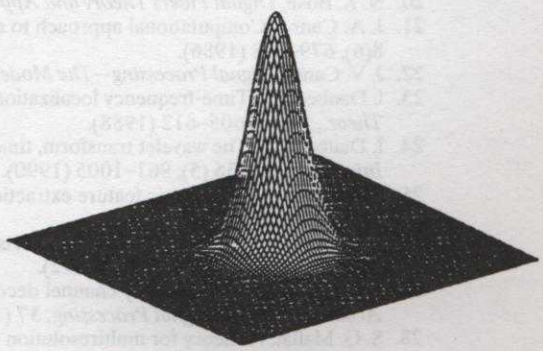

Fig. 11. The Gaussian.

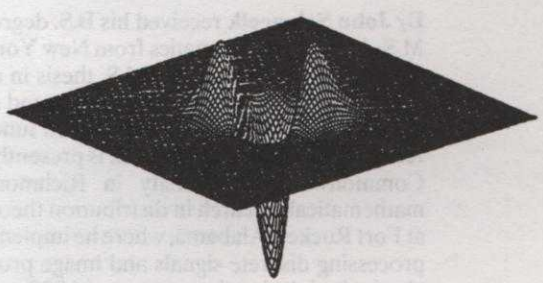

Fig. 12. Mother wavelet generated from Gaussian.

7. CONCLUSIONS

We have had a guided tour of profound mathematical concepts involving complex variables, transforms implementing improper integrals containing complex valued kernels, and directional derivatives to include gradients. It is the hope of the author that students having had the opportunity to explore the above visual examples incorporating these mathematical notions are now able to transport this learning experience to other relevant applications. The versatility of a student's ability to transport mathematical techniques to other situations is a major measure of their success in all fields of science.

REFERENCES

1. F. W. Campbell and J. G. Robson, Application of Fourier analysis to the visibility of gradings, *J. Physiol.*, **197**, 551–566 (1968).
2. J. M. Combes, A. Grossman and P. H. Tchamitchian (eds), Wavelets time–frequency methods and phase space. *Proc. of the International Conf.*, Marseille, France.
3. R. C. Gonzalez and R. E. Woods, *Digital Image Processing*, Addison-Wesley, Reading, M.A. (1992).
4. A. K. Jain, *Fundamentals of Digital Image Processing*, Prentice Hall, Englewood Cliffs, N.J. (1989).
5. A. Papoulis, *Signal Analysis*, McGraw Hill, New York (1977).
6. J. S. Lim, *Two-Dimensional Signal and Image Processing*, Prentice Hall, Englewood Cliffs, N.J. (1990).
7. A. Oppenheim and R. Schafer, *Digital Signal Processing*, Prentice Hall, Englewood Cliffs, N.J. (1975).
8. W. K. Pratt, *Digital Image Processing*, Wiley, New York (1991).
9. A. Rosenfield, Survey image analysis and computer vision: 1990, **53** (3), 322–365 (1991).
10. S. G. Mallat, Zero-crossing of a wavelet transform, *IEEE Trans. Inform. Theory*, **37** (4), 1019–1033 (1991).
11. D. Marr and E. Hildreth, Theory of edge detection, *Proc. R. Soc. Lond.*, B **207**, 187–217 (1980).
12. H. C. Andrews and B. R. Hunt, *Digital Image Restoration*, Prentice Hall, Englewood Cliffs, N.J. (1977).
13. D. H. Ballard and C. M. Brown, *Computer Vision*, Prentice-Hall, Englewood Cliffs, N.J. (1982).
14. R. M. Mersereau and D. E. Dudgeon, Two-dimensional digital filtering, *Proc. IEEE*, **63** (4), 610–623 (1975).
15. C. K. Chui (ed.), *An Introduction to Wavelets*, Vol. 1, Academic Press, New York (1992).
16. C. K. Chui (ed.), *Wavelets: A Tutorial in Theory and Applications*, Academic Press, New York (1992).
17. I. Daubechies, *Ten Lectures on Wavelets*, Society for Industrial and Applied Mathematics, P.A. (1982).
18. M. Ruskai, G. Beylkin, R. Coifman, I. Daubechies, S. Mallat, Y. Meyer and L. Raphael (eds) *Wavelets and Their Applications*, Jones and Bartlett, Boston, M.A. (1992).
19. B. G. Batchelor, *Pattern Recognition*, Plenum Press, New York (1978).
20. N. K. Bose, *Digital Filters Theory and Applications*, Elsevier, New York (1985).
21. J. A. Canny, Computational approach to edge detection, *IEEE Trans. Pattern Anal. Mach. Intell.*, **8**(6), 679–698 (1986).
22. J. V. Candy, *Signal Processing—The Modern Approach*, McGraw-Hill, New York (1988).
23. I. Daubechies, Time-frequency localization operators: A geometric approach, *IEEE Trans. Inform. Theor.*, **34** (4), 605–612 (1988).
24. I. Daubechies, The wavelet transform, time frequency localization and signal analysis, *IEEE Trans. Inform. Theor.*, **36** (5), 961–1005 (1990).
25. Zi-Quan Hong, Algebraic feature extraction of image for recognition, *Pattern Recognition*, **24** (3), 211–219 (1991).
26. G. Kaiser, An algebraic theory of wavelets, I. Operational calculus and complex structure, *SIAM J. Math. Anal.*, **23** (1), 222–243 (1992).
27. S. G. Mallat, Multifrequency channel decompositions of images and wavelet models, *IEEE Trans. Acoustics, Speech, Signal Processing*, **37** (12), 2091–2110 (1989).
28. S. G. Mallat, A theory for multiresolution signal decomposition: The wavelet representation, *IEEE Trans. Pattern Analysis Machine Intell.*, **11** (7), 674–693 (1989).
29. A. D. Poularikas and S. Selly, *Signals and Systems*, Prindle Weber & Schmidt, MA.. (1985).

Dr John Schmeelk received his B.S. degree in education from Seton Hall University and his M.S. degree in mathematics from New York University. While at N.Y.U., he worked under Dr Herbert Keller, writing his M.S. thesis in applied mathematics. He was then a captain in the U.S. Army Signal Corp for two years and served in Vietnam. Dr T. P. G. Liverman served as his advisor in the area of generalized functions at George Washington University where he received his Ph.D. Dr Schmeelk is presently an Associate Professor of mathematics at Virginia Commonwealth University in Richmond, Virginia, where he is engaged in applied mathematical research in distribution theory. He has spent the summers of 1986, 1988–1992 at Fort Rucker, Alabama, where he implemented procedures utilizing generalized functions in processing discrete signals and image processing to include human vision research. He was also invited during the summer of 1987 to contribute to an international generalized function seminar held in Dubrovnik, Yugoslavia and again in Varanasi, India during the winter of 1991.

He was an invited speaker at the International Partial Differential Equations Seminar held during the summer of 1993 in Plovdiv, Bulgaria. Dr. Schmeelk is a member of ASEE, MAA, AMS and is serving as Director in ASEE, Mathematics Division.